NURETH14-259

AN INTEGRAL EFFECT TEST ON THE FEEDWATER LINE BREAK OF APR1400 WITH THE ATLAS FACILITY

H. S. Park¹, S. Cho¹, K. H. Kang¹, Y. S. Kim¹, and K. Y. Choi¹

¹ Thermal Hydraulics Safety Research Division, Korea Atomic Energy Research Institute 1045 Daedeokdaero, Yuseong, Daejeon, 305-353, Korea

hspark@kaeri.re.kr, scho@kaeri.re.kr, khkang@kaeri.re.kr, yskim3@kaeri.re.kr, kychoi@kaeri.re.kr

Abstract

An integral effect test on the feedwater line break (FLB) was performed with the ATLAS facility for an APR1400 as a typical secondary system transient. The objectives of the present FLB tests are to understand the accident progression of the FLB scenario based on the APR1400 preliminary safety analysis report (PSAR) and to assess the prediction capability of system analysis codes such as the MARS, RELAP5, TRACE and SPACE. The main concern of the present FLB test is the peak RCS pressure and the major parameters affecting the peak RCS pressure are the break size, the break location, potential for reverse flow, initial pressurizer level and the initial SG level. The present test is performed for a break on the pipe connected to the economizer with a typical break size. The initial steady-state conditions and the sequence of event of FLB scenario for the APR1400 were successfully simulated with the ATLAS facility. In the present paper, major thermal-hydraulic phenomena such as the system pressures, the collapsed water levels, and the break flow rate are presented and discussed. It could be concluded that the APR1400 has the capability of coping with the hypothetical FLB scenario with an adequate set of controlling devices and proper setpoints. This integral effect test data could also be used to evaluate the prediction capability of existing safety analysis codes of MARS, RELAP5 and SPACE and to identify any code deficiency for an FLB simulation.

1. Introduction

An integral effect test for a feedwater line break (FLB) was performed with the ATLAS (Advanced Thermal-Hydraulic Test Loop for Accident Simulation) [1] by KAERI (Korea Atomic Energy Research Institute).

1.1 Background

The FLB accident is one of the typical secondary system transients and it is categorized as one of the transient accidents which cause the decrease of the heat removal from the secondary system. [2] Although FLB accidents are not expected to occur often in pressurized water reactor (PWR) plants, the potential for the primary system pressure boundary to rupture due to over-pressurization necessitates their examination. [3]

When the FLB occurs, the feedwater terminates and the affected steam generator (SG) inventory decreases. As the pressure and temperature of an intact SG increase, the reactor coolant system (RCS) temperature increases, the swollen water inventory insurges to the pressurizer to increase its level, and the RCS pressure increases to generate a high pressurizer pressure (HPP) trip. When the pressurizer is over-pressurized, the pressurizer safety valve (PSV) is open to mitigate the pressure increase in the primary system. As the secondary system is pressurized, the main steam safety valves (MSSVs) are open to mitigate the pressure increase in the secondary system and the water inventory decreases gradually. As the pressure of intact SG decreases to a certain setpoint, the main steam isolation signal (MSIS) is generated with a certain delay, after which the main steam isolation valves (MSIVs) and the main feedwater isolation valves (MFIVs) are closed. While the affected SG is rapidly depressurized after the isolation of SGs, the pressure of intact SG is fluctuated with the operation of MSSVs and the auxiliary feedwater pump (AFP). As the level of intact SG decreases to a certain setpoint, the AFP is actuated. As the level of intact SG increases to a certain setpoint, the AFP stops. The plant could be cooled down slowly with the continuation of this process.

1.2 Objectives

With the aim of providing integral effect test data to validate the SPACE code [4, 5], it was decided to perform two tests, namely the FLB-EC-01 and FLB-DC-01, in technical consultation with the Korean nuclear industry. In order to investigate the effects of the break location on the transient thermal-hydraulic behavior, two cases for breaks on the pipes connected to the SG economizer and down-comer have finally been selected as the representative cases to validate the SPACE code.

In this study, the FLB-EC-01 test was performed to simulate a break on the pipe connected to the SG economizer with a typical break size. In the FLB-EC-01 test, a break on the pipe connected to the economizer with a typical break size of 0.4 ft² (APR1400-based size) was simulated. With the aim of simulating the FLB accident of the APR1400 as realistically as possible, a pertinent scaling approach was taken. The main objectives of this test were not only to provide some physical insight into the system response of the APR1400 during the FLB accident but also to produce integral effect test data to validate the SPACE code.

2. Description of the ATLAS facility

ATLAS has the same two-loop features as the APR1400 and is designed according to the well-known scaling methodology suggested by Ishii and Kataoka [6] to simulate the various test scenarios as realistically as possible. The ATLAS is a half-height and 1/288-volume scaled test facility with respect to the APR1400. The main motive for adopting the reduced-height design is to allow for an integrated annular down-comer where the multidimensional phenomena can be important in some accident conditions with a DVI operation. According to the scaling law, the reduced height scaling has time-reducing results in the model. For the one-half-height facility, the time for the scaled model is $\sqrt{2}$ times faster than the prototypical time. The friction factors in the scaled model are maintained the same as those of the prototype. The major scaling parameters of the ATLAS are summarized in Table 1.

A schematic diagram of the ATLAS is shown in Fig. 1. The fluid system of the ATLAS consists of a primary system, a secondary system, a safety injection system, a break simulating system, a containment simulator, and auxiliary systems. The primary system includes a reactor vessel, two hot legs, four cold legs, four intermediate legs, a pressurizer, four reactor coolant pumps, and two steam generators. The secondary system of the ATLAS is simplified to be of a circulating loop-type. The steam generated at two steam generators is condensed in a direct condenser tank and the condensed feed-water is again injected into the steam generators. Most of the safety injection features of the APR1400 and the OPR1000 are incorporated into the safety injection system of the ATLAS. It consists of four SITs (Safety Injection Tanks), a high pressure SIP which can simulate safety injection and long-term cooling, a charging pump for charging auxiliary spray, and a shutdown cooling pump and a shutdown heat exchanger for low pressure safety injection, shutdown cooling operation and recirculation operation. The break simulation system consists of several break simulating lines such as the LBLOCA, DVI line break LOCA, SBLOCA, SGTR, MSLB and FLB, etc. Each break simulating line consists of a quick opening valve, a break nozzle and instruments. It is precisely manufactured to have a scaled break flow rate in the case of LOCA tests. The CS (Containment Simulator) of the ATLAS has the function of collecting the break flow and maintaining a specified back-pressure in order to simulate containment pressure. The CS is mainly composed of two separating vessels, five measuring vessels to measure the accumulated water mass, a flow meter to measure the steam flow rate and a pressure control valve to control the containment pressure. Besides, the ATLAS has some auxiliary systems such as a makeup water system, a component cooling water system, a nitrogen/air/steam supply system, a vacuum system, and a heat tracing system.

Table 1 Major scaling parameters of the ATLAS

Parameters	Scaling law	ATLAS design
Length	l_{0R}	1/2
Diameter	$d_{_{0R}}$	1/12
Area	d_{0R}^{2}	1/144
Volume	$l_{0R}d_{0R}^{2}$	1/288
Core DT	ΔT_{0R}	1
Velocity	$l_{0R}^{1/2}$	$1/\sqrt{2}$
Time	$l_{0R}^{1/2}$	$1/\sqrt{2}$
Power/Volume	$l_{0R}^{-1/2}$	$\sqrt{2}$
Heat flux	$l_{0R}^{-1/2}$	$\sqrt{2}$
Core power	$l_{oR}^{1/2}d_{0R}^{2}$	1/203.6
Flow rate	$l_{oR}^{1/2}d_{0R}^{2}$	1/203.6
Pressure drop	l_{0R}	1/2

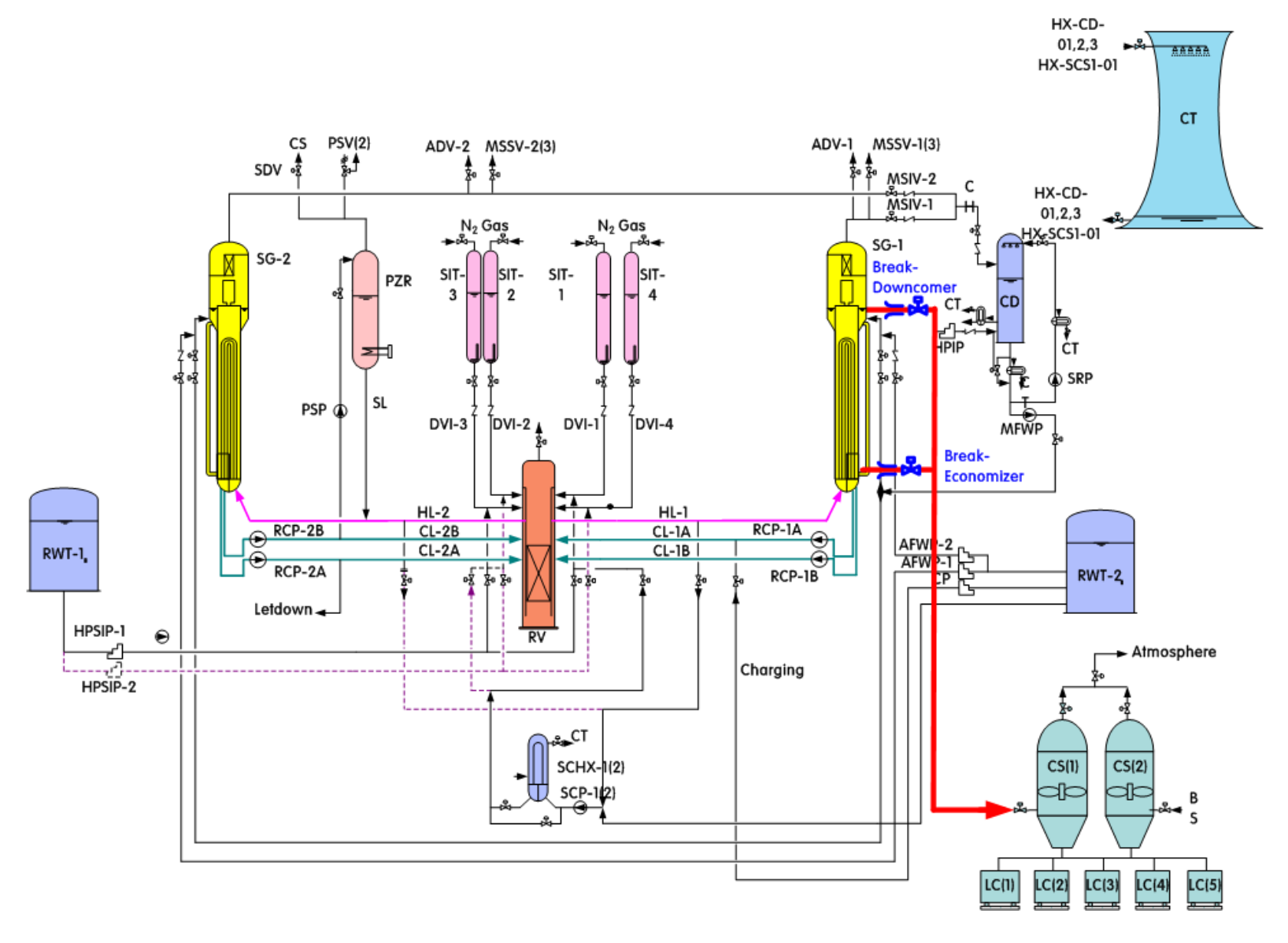


Figure 1 A schematic diagram of the ATLAS

A total of 396 electrical heaters and unheated rods are used to simulate the fuel rods. There are 390 electric heaters which are divided concentrically into 3 groups (Group-1, Group-2 and Group-3). Group-1, -2, and -3 heaters are located in the inner, middle, and outer regions of the heater bundle, respectively, and they have 102, 138 and 150 heaters, respectively. In addition to that the core heater bundle has 6 unheated rods. The axial power profile of each heater rod is the 'chopped cosine' power shape. The simulated fuel assembly type is 16×16 and the outer diameter of a heater rod is 9.5 mm, which is the same as the prototypical rod diameter of APR1400. A total of 264 and 42 thermocouples were installed in the core heater bundle to measure the heater surface and fluid temperatures, respectively, which were inserted into grooves on the heater rod surface.

The ATLAS has two steam generators and each steam generator consists of a lower plenum, a Utube assembly, middle and upper steam generator vessels, two down-comer pipes, and other internals as shown in Fig. 2. The whole parts of the steam generator are made of stainless steel (SA 240-316) except for the U-tubes which are made of stainless steel (SA 213-TP347). The lower plenum of the steam generator is composed of a cylindrical body with a hemispherical head, 1 hotleg and 2 intermediate-leg nozzles, a divider plate as a barrier between the inlet and the outlet plenums, and a connecting flange. The U-tube assembly consists of a tube sheet, an economizer divider plate, 8 tube support plates, and 176 U-tubes. The tube sheet is installed between the lower plenum and the middle steam generator vessel, and it serves as a physical boundary between the primary and the secondary systems. The outer diameter, thickness and averaged length of a U-tube are 14.2 mm, 1.1 mm and 9.2462 m, respectively.

The detailed ATLAS design and a description of the ATLAS development program can be found in the literature. [7-8]. A detailed description of the signal processing system and control system of the ATLAS can also be found in the literature. [9-10] In the ATLAS test facility, a total of 1,236 instruments are installed for the measurement of the thermal-hydraulic parameters in the components.

The uncertainty of the measured experimental data was analysed in accordance with a 95% confidence level. According to the ASME performance test codes 19.1, the uncertainty interval of the present results was given by the root-mean-square of a bias contribution and a precision contribution [11]. The bias and precision errors were evaluated from the data acquisition hardware specifications and the calibration results performed once every year, respectively. Table 2 shows the analysed uncertainty levels of each group of instruments.

Table 2 Uncertainty levels of instruments

Items	Unit	Uncertainty
Static Pressure	MPa	0.56%
Differential Pressure	kPa	0.46%
Collapsed Water Level	m	2.21%
Temperature	°C	maximum 2.4 °C
Flow rate	kg/s	2.65%

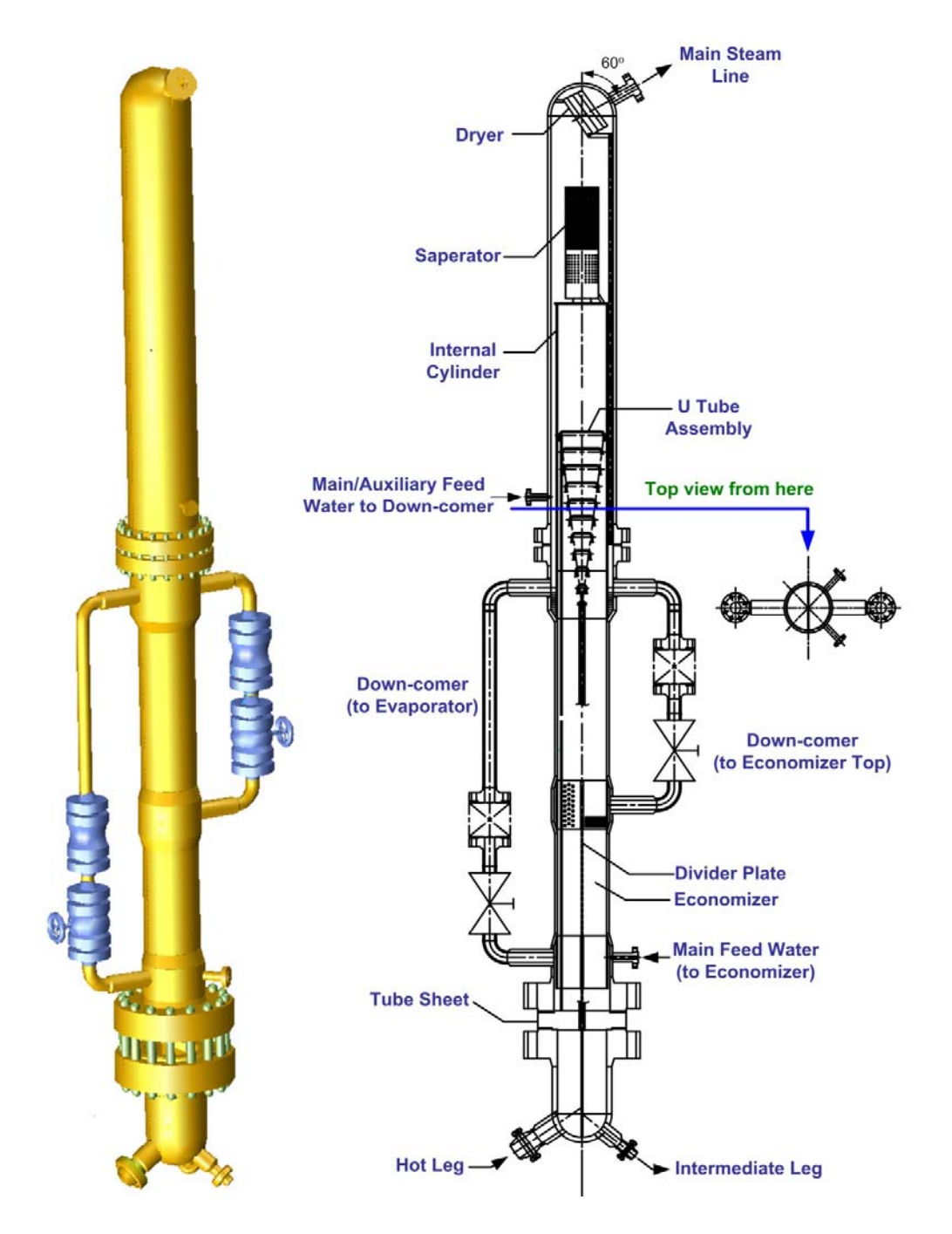


Figure 2 Steam generator of the ATLAS.

3. Experimental conditions and procedures

The FLB-EC-01 test was performed to simulate a break on the pipe connected to the economizer of an affected steam generator (SG-1) as shown in Fig. 3. In the present FLB-EC-01 test, considering the safety analysis results for the FLB accident of the APR1400 [12], a reactor trip was assumed to occur at a pre-determined time. The trip time was determined based on the time when the HPP trip occurred in the APR1400 after the break.

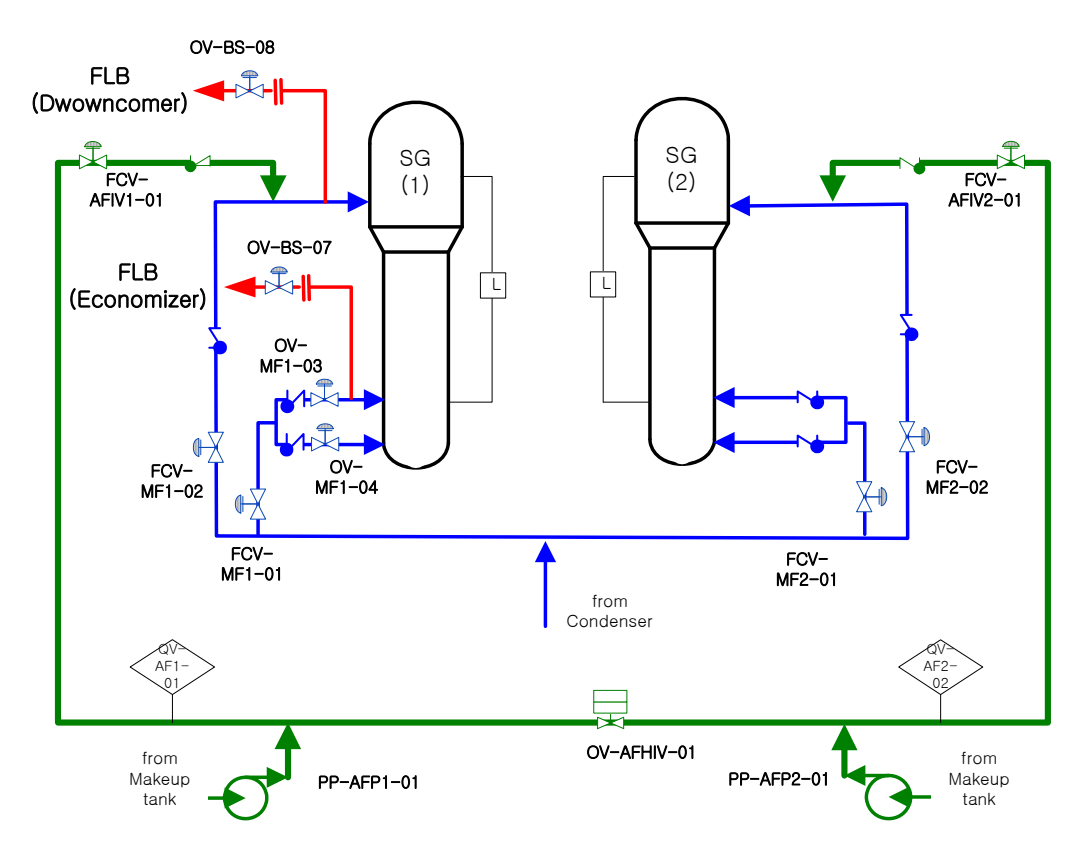


Figure 3 Piping arrangement of break simulation system for feedwater line break.

3.1 Test conditions

3.1.1 Break nozzle design

In order to simulate an FLB accident of the APR1400 as realistically as possible, a boundary flow scaling approach was taken from a break flow rate point of view. During the FLB, the break flow can be choked or it is not depending on the differential pressure between the primary system and the atmosphere. In either case, the break flow rate in the ATLAS should be scaled down appropriately with respect to the APR1400. Based on the boundary flow scaling criteria, the break flow rate should be preserved according to Eq. (1). Taking into account the velocity scaling ratio of the ATLAS, i.e., $u_R = l_{oR}^{1/2}$, Eq. (1) can be expressed as Eq. (2).

$$\left[\frac{a_{break}}{a_o} \frac{u_{break}}{u_o}\right]_R = 1, \tag{1}$$

The 14th International Topical Meeting on Nuclear Reactor Thermalhydraulics, NURETH-14 Toronto, Ontario, Canada, September 25-30, 2011

$$\left[\frac{a_{break}}{a_o}\right]_{R} u_{break,R} = u_{oR} = l_{oR}^{1/2}, \tag{2}$$

The break flow is determined by the choking flow. As for the choking flow, the velocity ratio of the break flow ($u_{break,R}$) becomes one. And as for the non-choking flow, the break flow is determined by the differential pressure between the primary system and the atmosphere. Thus, the velocity ratio of the break flow can be expressed as in Eqs. (3) and (4) for choking and non-choking flow cases, respectively.

Choking flow condition:
$$u_{break,R} = 1$$
, (3)

Non-choking flow condition:
$$u_{break,R} = \left[f \frac{l}{d} + K \right]_{R}^{-1/2} \cdot \Delta P_{R}^{1/2}$$
. (4)

Finally, in order to preserve the break flow rate, from Eqs. (2), (3) and (4), the break area in the ATLAS test should be scaled down with respect to the APR1400 as in Eqs. (5) and (6) for choking and non-choking flow cases, respectively.

Choking flow condition:
$$a_{break,R} = a_{oR} l_{oR}^{1/2}$$
, (5)

Non-choking flow condition:
$$a_{break,R} = a_{oR} l_{oR}^{1/2} \cdot \left[f \frac{l}{d} + K \right]_{R}^{1/2} \cdot \Delta P_{R}^{-1/2}$$
. (6)

According to the scaling factor of the ATLAS, a break area ratio becomes 1/203.6 if a choking flow condition is assumed. On the other hand, since the velocity decreases by a factor of $\sqrt{2}$ due to the half-height scale of the ATLAS, the pressure loss coefficient [f l/d + K] should be double the prototypic value in the test, if a non-choking flow condition is assumed.

The target scenario of the present study is the break on the pipe connected to the economizer with a typical size of 0.4 ft² in the APR1400. Figure 3 shows the piping arrangement of the break simulation system which consists of a break simulation valve (OV-BS-07) having an opening time of 0.25 seconds and a break nozzle. The inner diameter of a break nozzle for the present test was obtained to be 15.24 mm. As for the selected diameter of the break tube, the length of the break tube was determined to be

193 mm in order to preserve the break flow rate for the non-choking flow condition. The length was determined to be approximately 12 times the inner diameter following the long pipe assumption. [13]

3.1.2 <u>Determination of Test Conditions</u>

The present test conditions were determined by a pre-test calculation with a best-estimate thermal-hydraulic safety analysis code, MARS-KS [14]. First of all, a transient calculation was performed for a break on the pipe connected to the SG economizer of the APR1400 to obtain the initial reference and boundary conditions. A best-estimate safety analysis methodology, which is now commonly accepted in the nuclear industry, was applied to the transient calculation of the APR1400. A single failure assumption for a safety injection system was assumed in the MARS calculation; four SITs and two of the four SIPs were available. The initial and boundary conditions for the present test were obtained by applying the scaling ratios shown in Table 1 to the MARS calculation results for the APR1400 [15]. Table 3 compares the steady-state conditions between the APR1400 and the ATLAS for the present test. The actual initial conditions of the FLB-EC-01 test were also summarized in the Table.

Table 3 Calculated and actual initial conditions for the FLB-EC-01 test

	APR1400	Design		FLB-EC-01 test	
Design parameters (steady- state)		Values	Instrument	Values	Standard deviation
Reactor Pressure Vessel					
Normal power (MWt)	3983	1.56	Power-Total	1.640	0.001
Pressurizer pressure (MPa)	15.5	15.5	PT-PZR-01	15.53	0.0014
Core inlet temperature (°C)	291.3	290.7	TF-LP-02G18	290.25	0.175
Core outlet temperature (°C)	324.2	324.2	TF-CO-07G25	324.59	0.275
Pressurizer level (m, Full)	-	-	LT-PZR-01	4.332	0.0087
Steam Generator (SG-1, SG-2	2)				
Steam pressure (MPa)	6.9	7.83	PT-SGSD1-01 PT-SGSD2-01	7.795 7.795	0.001 0.001
Steam temperature (°C)	284.9	293.5	TF-SGSD1-03 TF-SGSD2-03	295.2 295.3	0.083 0.072
Steam flow rate (kg/s)	1152.4	0.444	QV-MS1-01 QV-MS2-01	0.398 0.432	0.001 0.001
Feed water flow rate (kg/s)	1152.4	0.444	QV-MF1-01,02 QV-MF2-01,02	0.388, 0.052 0.392, 0.042	0.00055, 0.00005 0.00047, 0.00020
Feed water temperature (°C)	232.2	232.2	TF-MF1-01 TF-MF2-01	234.6 234.6	0.13 0.14
SG water level (m, WR)	-	-	LT-SGSDRS1-01 LT-SGSDRS2-01	4.82 4.99	0.007 0.008
Primary Piping (HL-1, HL-2)					

The 14th International Topical Meeting on Nuclear Reactor Thermalhydraulics, NURETH-14 Toronto, Ontario, Canada, September 25-30, 2011

Hot leg flow (kg/s)	11080.2	4.0	QV-HL1-01B QV-HL2-01B	3.69 4.36	0.410 0.185
Hot leg temperature (°C)	323.3	323.8	TF-HL1-03A TF-HL2-03A	324.8 6	0.252 0.111
Primary Piping (CL-1A, CL-1B, CL-2A, CL-2B)					
Cold leg flow (kg/s)	5540.1	2.0	QV-CL1A-01B QV-CL1B-01B QV-CL2A-01B QV-CL2B-01B	2.08 2.29 2.27 2.08	0.068 0.058 0.044 0.057
Cold leg temperature (°C)	291.3	289.9	TF-CL1A-04A TF-CL1B-04A TF-CL2A-04A TF-CL2B-04A	292.29 292.15 291.29 292.53	0.189 0.107 0.119 0.250

The decay heat was simulated to be 1.2 times that of the ANS-73 decay curve for conservative conditions. The initial heater power was controlled to be maintained at about 1.645 MW, which was equal to the sum of the scaled-down core power (1.565 MW) and the heat loss rate of the primary system (about 80 kW). The heater power was then controlled to follow the specified decay curve after 10.6 seconds from the opening of the break simulation valve (OV-BS-07). In the FLB-EC-01 test, the uniform radial power distribution was applied. Figure 4 shows the initial power level and the decay power variation during the FLB-EC-01 test. During the test period, the heat loss rate of the primary loop was estimated to be about 80 kW, and the heat loss through two steam generators was about 60 kW [16].

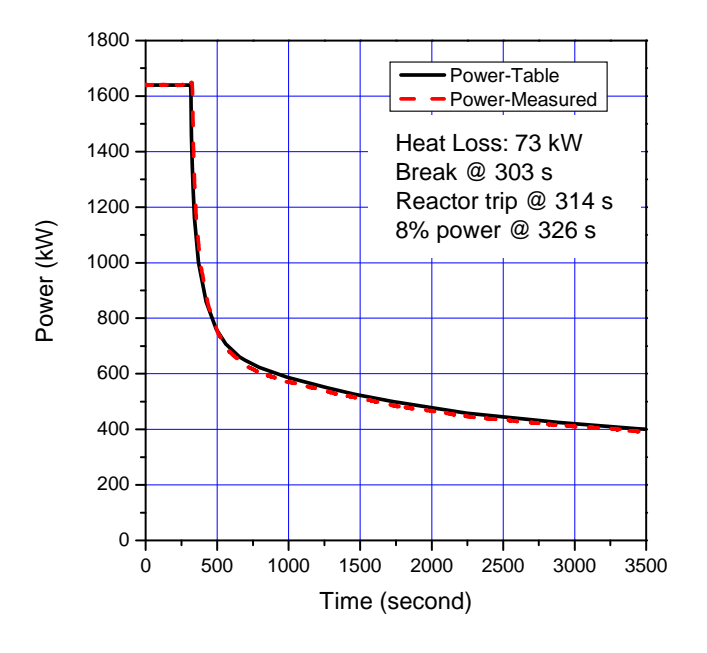


Figure 4 Applied core power.

In addition, a single-failure such as the loss of a diesel generator, resulting in the minimum safety injection flow to the reactor pressure vessel, was assumed to occur in concurrence with the reactor trip. Therefore, the safety injection water from the SIP was only available through the DVI-1 and -3 nozzles, and the safety injection water from the SIT was available through all of the DVI nozzles.

3.2 Test procedures

Prior to a main test, several actions should be taken to set proper initial and boundary conditions. Such actions include the instrument calibration, purging and filling the ATLAS system including leakage tests, and the implementation of test-specific control logics into the process control computers for sequence control. The sequence control logics execute the required control actions for the corresponding control devices such as the main core heater, reactor coolant pump (RCP), SIP, and valves. Detailed descriptions of the test procedures can be found in the literature [17].

When the whole system had reached a specified initial condition for the test, as shown in Table 3, the steady-state conditions of the primary and the secondary systems were maintained for more than 30 minutes. After this steady-state period, the main test was started by opening the break simulation valve, OV-BS-07. Coincidently with the break, the main feedwater pumps stopped and the main feedwater isolation signal (MFIS) was generated to close the main feedwater isolation valves (MFIVs). For the reactor trip to be induced, the HPP trip signal was set to be actuated 10.6 seconds after the reactor break. This HPP trip signal was adjusted to be generated at the scaled time of the APR1400. It is because the ATLAS facility has a maximum 10% capacity of the scaled full power that the primary system could not be pressurized to reach a HPP signal.

When the HPP trip signal occurred, both the RCP and the turbine stopped simultaneously. The pressurizer heater was also tripped with the HPP trip signal. The main steam isolation valves (MSIVs) were closed 4.56 seconds after the low SG pressure (LSGP) signal. The closing of the MFIVs and the MSIV is equivalent to the containment isolation of the APR1400. As the primary system pressure was always maintained higher than the actuation setpoint of the SIP (10.7244 MPa) during the present FLB-EC-01 test period, neither the SIP water nor the SIT water was supplied.

The water level of the affected steam generator (SG-1) decreased rapidly to empty. Contrary to the SG-1, the water level of the intact steam generator (SG-2) decreased continuously and reached the set-point of the auxiliary feedwater actuation signal (AFAS). An injection of the auxiliary feedwater recovered the water level of the SG-2. Figure 5 shows the injected auxiliary feedwater flow rate and the accumulated mass during the FLB-EC-01 test period. Table 4 shows the sequence of events observed in the present FLB-EC-01 test.

Table 4 Actual sequence of events of the FLB-EC-01 test

Event	Time - DAS (second)	Time after Break (second)	Remarks (Set-point)
Break opening	303	0	
Main feedwater stop & MFIS	303	0	Coincidently with the break
HPP signal	314	11	10.6 s after break
Reactor trip (Decay power	314	11	HPP + 0.071 s
RCP trip	314	11	Coincidently with the reactor
Turbine trip	314	11	Coincidently with the reactor
MSSV opening	339, 401 (SG-1) 339, 401, 775, 926, 1601 (SG-2)	36, 98 (SG-1) 36, 98, 472, 623, 1298 (SG-2)	PT-SGSD1,2-01 @ 8.1 MPa (opening) PT-SGSD1,2-01 @ 8.1 MPa (closing)
LSGP signal	456	153	PT-SGSD1-01 @ 5.895 MPa
MSIS	461	158	LSGP + 4.56 s
PSV opening	Not actuated	Not actuated	PT-PZR-01 @ 17.03 MPa
AFAS on/off (SG-2)	975/1197, 1277/1361, 1423/1528, 1468/2007,	672/894, 974/1058, 1120/1225, 1165/1704,	LT-SGSDRS2-01 level = 2.78 m / 3.9 m (Actually LT-SGSDRS2-01 < 3.9 m)
LPP signal	Not actuated	Not actuated	PT-PZR-01 @ 10.7244 MPa
SIP injection	Not actuated	Not actuated	LPP + 28.28 s delay
SIT injection	Not actuated	Not actuated	PT-PZR-01 < 4.03 MPa

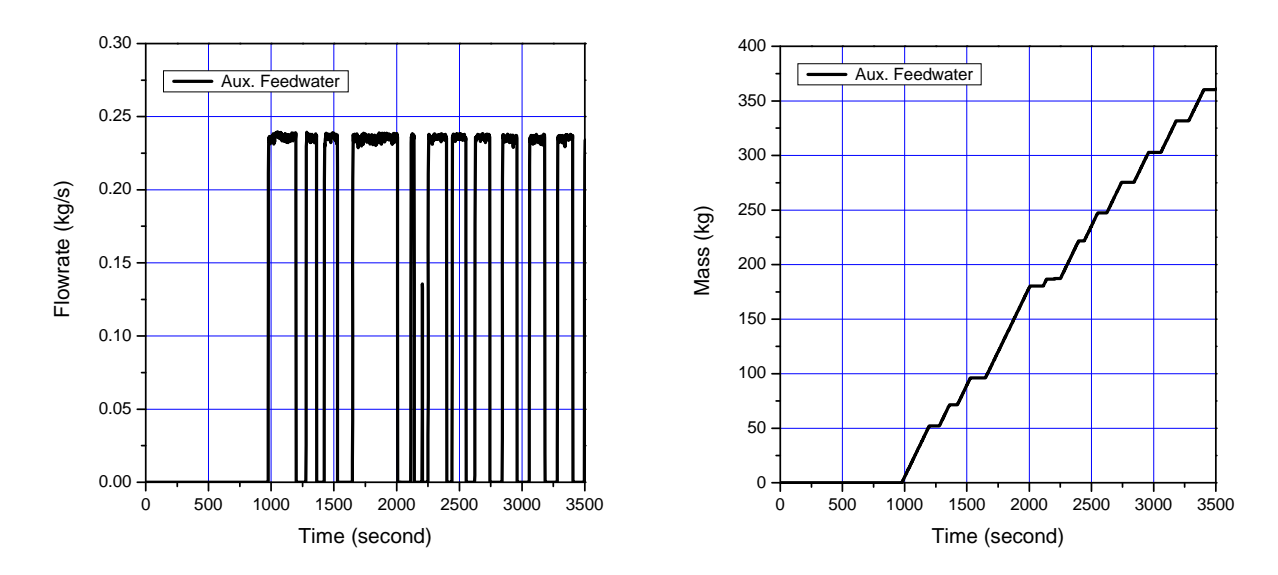


Figure 5 Injected auxiliary feedwater flow rate and accumulated mass.

4. Discussions on the experimental results

For the FLB-EC-01 test the steady-state data was successfully acquired for major scaling parameters as shown in Table 3 and the actual sequence of event was also successfully simulated as shown in Table 4.

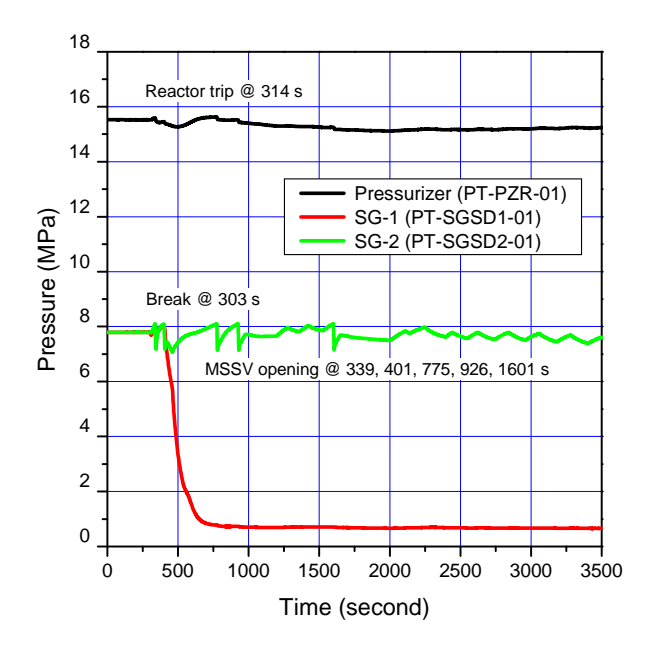
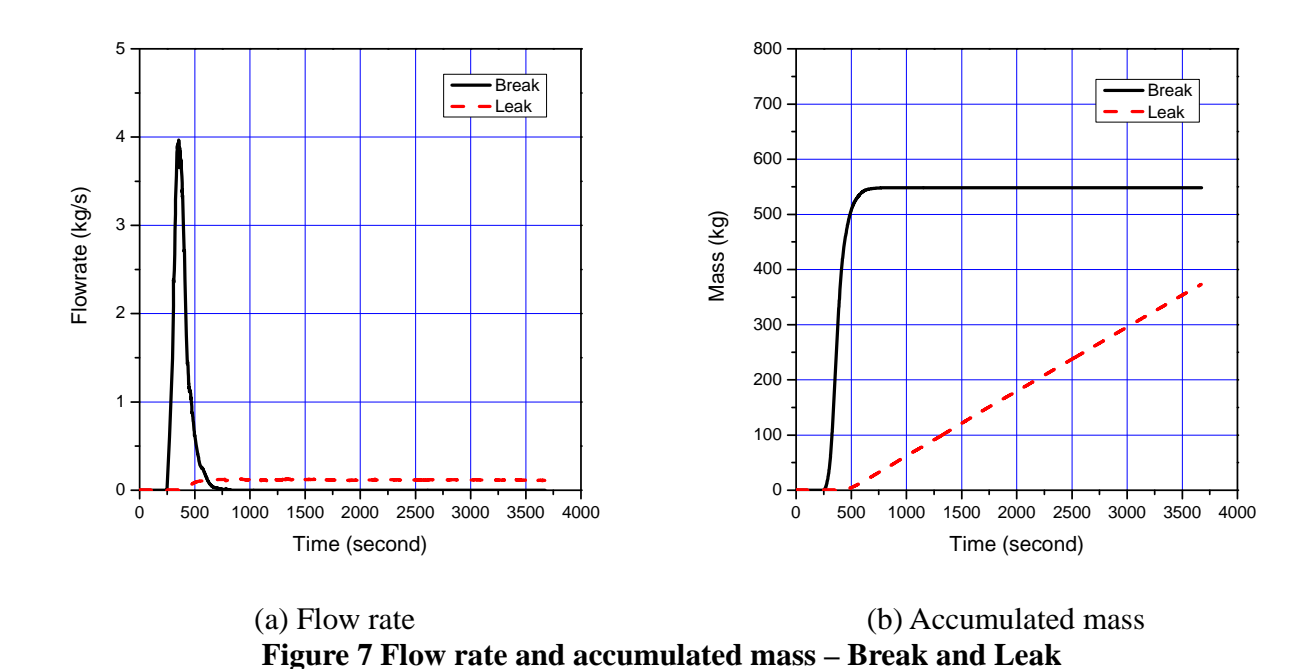


Figure 6 Pressure trend at the pressurizer and the steam generator steam dome.

Figure 6 shows the pressure trend at the pressurizer and the steam generator steam dome. When the FLB event was initiated by opening the break simulation valve, OV-BS-07, the affected SG was depressurized very rapidly. The main feedwater pump stopped and the main feedwater was isolated simultaneously with the break. The HPP trip signal was actuated 10.6 seconds after the break, which was generated at the scaled time of the reactor trip in the APR1400 simulation. It should be noted that the arbitrary generation of HPP trip signal was due to the low power capacity of ATLAS, maximum 8% of scaled full power. With the low power of 8% instead of 100%, the primary pressure increases very little before the trip. The primary temperature shows the similar trend, as shown in Fig. 11.

The reactor tripped 0.071 s after the HPP and both the RCP and the turbine tripped simultaneously. Following the turbine trip, the secondary system pressure increased until the MSSVs were opened to reduce the secondary system pressure. The first opening time of the MSSVs both in SG-1 and SG-2 was 339 seconds from the DAS start, which was 36 seconds after the beginning of the FLB transient. Subsequent to the peak in the secondary system pressure of the steam generators, the secondary system pressure decreased, resulting in the temporary closure of the MSSVs. Then, the secondary system pressure started to increase again until it reached the MSSV set-point, resulting in the second opening of the MSSVs both in SG-1 and SG-2. After the steam generators were isolated due to the MSIS actuations following the low steam generator pressure signal from the affected SG (SG-1), only the MSSVs in the intact steam generator (SG-2) were actuated. After the isolation, the pressure of the affected SG rapidly decreased and that of the intact SG increased again. The MSSVs of the intact SG were actuated twice before the injection of the auxiliary feedwater. The low SG pressure (LSGP) signal was generated when the SG steam dome pressure (PT-SGSD1-01) dropped below 5.895 MPa. The MSIVs began to close 4.56 s after the LSGP signal.



The auxiliary feedwater was injected into the intact SG on and off for the SG level to be below 3.9 m. It was due to the erroneous operation of the control logic. The secondary pressure of the SG-2 decreased during the injection of the auxiliary feedwater into the intact SG, but it increased without the

injection. After the auxiliary feedwater supply was terminated resulting from the recovery of the water level in the SG-2, the secondary pressure of the steam generators increased and then the MSSVs were opened again around 1601 s after the break. The variation of the auxiliary feedwater flow rate and the accumulated mass was shown in Figure 5. Although the primary system pressure was fluctuating a little after the break, it always remained above 15.0 MPa throughout the entire test as shown in Figure 6.

Figure 7 shows the variation of the break flow rate and the accumulated mass during the FLB-EC-01 test. The break flow rate was measured by using the containment simulator but there was some leak from the intact SG to the broken SG due to the failure of inter-connecting isolation valve. The leak flow rate was estimated from the pressure difference between two SGs and the calculated form loss coefficient of the connecting pipe, which was calculated based on the measured flow rate when only the leak flow existed during the later period. Initially the break flow rate increased to 4.0 kg/s and it decreased to zero around 825 s. The accumulated mass was around 548 kg during the FLB-EC-01 test. The maximum leak flow rate was about 0.12 kg/s and its accumulated mass was around 373 kg.

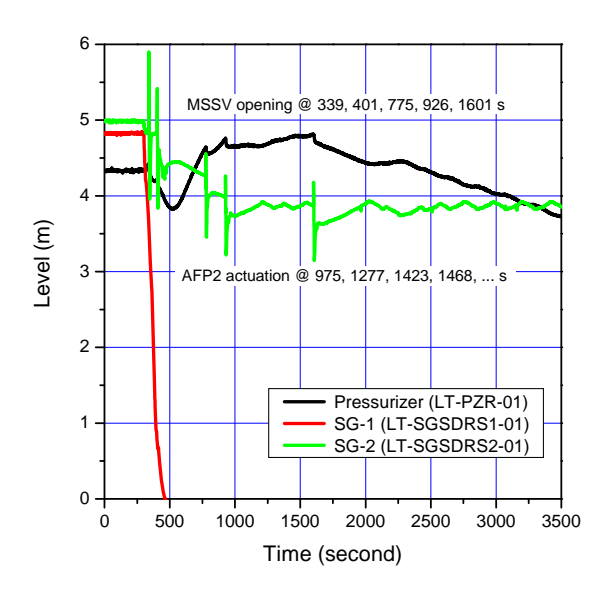


Figure 8 Collapsed water levels in the pressurizer and the SG secondary side.

Figure 8 shows the variation of the collapsed water level in the pressurizer and the secondary side of the steam generators. Due to the break flow, the collapsed water level showed a rapid decrease in the affected steam generator. The collapsed water level decreased to 3.9 m in the intact steam generator during which there were level fluctuations resulting from the discharged flow through the MSSVs. The supply of the auxiliary feedwater increased the water level of the intact steam generator. Contrary to the secondary side of the steam generators, the collapsed water level of the pressurizer continuously decreased to 3.83 m below the initial level (4.33 m), increased to 4.82 m and thereafter decreased steadily.

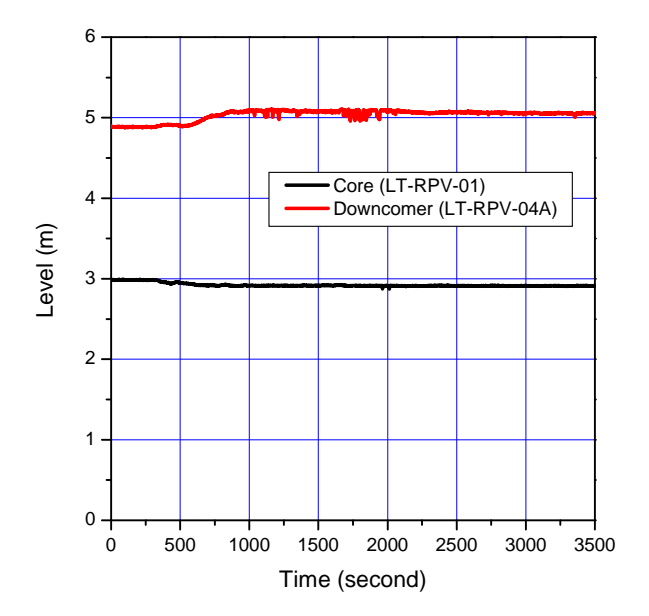


Figure 9 Collapsed water levels in the core and the down-comer.

Figure 9 shows the variation of the collapsed water levels in the core and the down-comer. The SI water was not injected into the down-comer during the whole test period and the levels in the core and the down-comer showed little fluctuation. Figure 10 shows the maximum cladding temperature behavior. No excursion in the cladding temperature was observed. Figure 11 shows the variation of the fluid temperatures in the primary coolant loops. When the break occurred, the fluid temperatures in the hot legs showed a sudden decrease due to the reduced core power after the trip. The fluid temperatures of the cold leg-2A and -2B maintained steady values but those of the cold leg-1A and -1B increased to just below the hot leg temperature. It was due to this fact that the affected SG was drained to be empty. The heat transfer through the affected SG was very small compared to that through the intact SG.

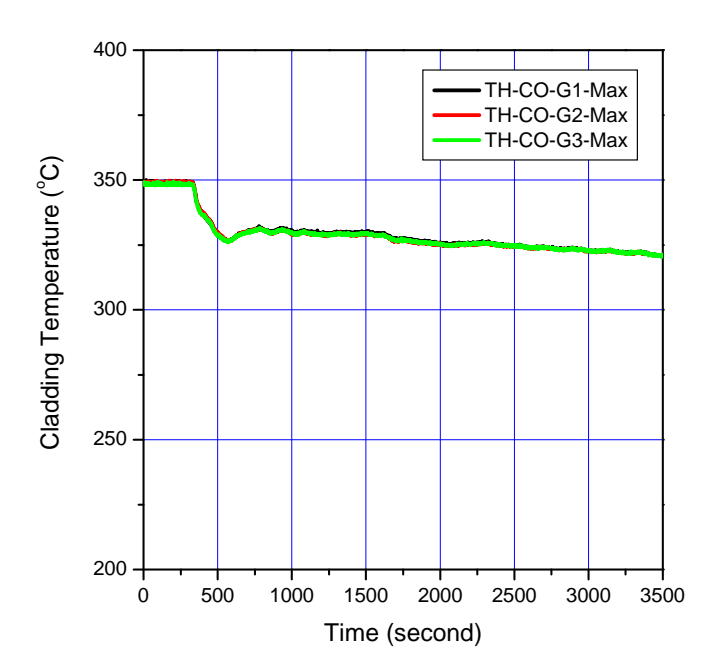


Figure 10 Maximum cladding temperatures.

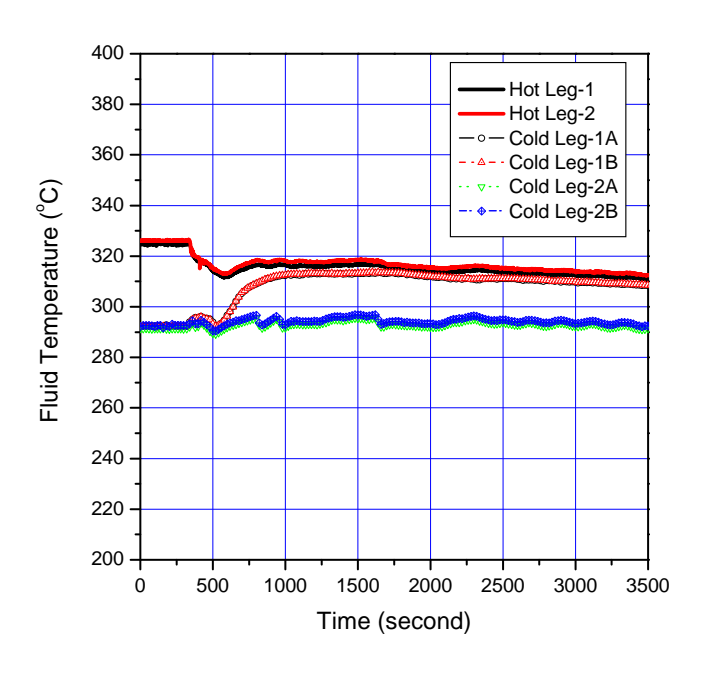


Figure 11 Fluid temperatures in the primary coolant loops.

5. Conclusion

The FLB-EC-01 test was performed with the ATLAS to simulate a break on the pipe connected to the SG economizer in the APR1400. The main objectives of this test were not only to provide a physical insight into the system response of the APR1400 during the FLB but also to produce integral effect experimental data to validate the SPACE code.

The initial steady-state conditions and the sequence of event of FLB scenario for the APR1400 were successfully simulated with the ATLAS facility. In the present paper, major thermal-hydraulic phenomena such as the system pressures, the collapsed water levels, and the break flow rate are presented and discussed. Following the reactor trip induced by a high pressurizer pressure, the feedwater supply was stopped and the secondary system pressure increased until the MSSVs opened after 36 seconds from the break to reduce the secondary system pressure. The MSSVs repeated their on and off status depending on the secondary system pressure during the whole test period. The primary system pressure maintained a steady value with very little fluctuation. A mild change of the water level in the core and down-comer was observed. No excursion in the cladding temperature was observed. The break flow rate was high up to 4.0 kg/s, initially, and it decreased to zero around 825 s.

It could be concluded that the APR1400 has the capability of coping with the hypothetical FLB scenario with an adequate set of controlling devices and proper setpoints. This integral effect test data could also be used to evaluate the prediction capability of existing safety analysis codes of MARS, RELAP5 and SPACE and to identify any code deficiency for an FLB simulation.

6. References

- [1] W.P. Baek, C.H. Song, B.J. Yun, et al. "KAERI Integral Effect Test Program and the ATLAS Design," Nuclear Technology, 152, 2005, p.183.
- [2] Korea Electric Power Corporation, "Preliminary Safety Analysis Report on Shin-Kori 3 & 4 Units," Chapter 15, 2008.
- [3] T. J. Boucher et al., "Results of SEMISCALE Mod-2C Feedwater and Steam Line Break(S-FS) Experiment Series: Bottom Main Feedwater Line Break Accident Experiments," NUREG/CR-4898, EGG-2503, EG&G Idaho, Inc, 1988.
- [4] D. H. Lee et al., "Overview of SPACE thermal-hydraulic analysis code development," NUTHOS-7, October 5-9, 2008, Seoul, Korea.
- [5] K. Y. Choi et al., "Development of a Wall-To-Fluid Heat Transfer Package for the SPACE Code," Nuclear Engineering and Technology, 41, No. 9, 2009, pp.1143-1156.
- [6] M. Ishii and I. Kataoka, "Similarity Analysis and Scaling Criteria for LWRs under Single Phase and Two-Phase Natural Circulation," NUREG/CR-3267, ANL-83-32, Argonne National Laboratory, USA, 1983.
- [7] H. S. Park, et al., "Calculation Sheet for the Basic Design of the ATLAS Fluid System," KAERI/TR-3333/2007, KAERI, Daejeon, Korea, 2007.

- [8] Y.S. Kim, K.Y. Choi, H.S. Park, S. Cho, B.D. Kim, N.H. Choi, W.P. Baek, "Commissioning of the ATLAS thermal-hydraulic integral test facility," Annals of Nuclear Energy, 35, 2008, pp. 1791-1799.
- [9] S. Cho et al., "Description of the Signal Processing System of ATLAS Facility," KAERI/TR-3334/2007, 2007.
- [10] K.Y. Choi et al., "Control and Data Acquisition System of the ATLAS Facility," KAERI/TR-3338/2007, Korea Atomic Energy Research Institute, 2007.
- [11] The American Society of Mechanical Engineers, "Test Uncertainty," ASME PTC 19.1-1998, 1998.
- [12] H.S., Park, et al., "Test Prospectus for the ATLAS Feedwater Line Break Tests. 53211-TP-FLB-EC-01, Rev. 00," Korea Atomic Energy Research Institute, 2010.
- [13] C.K., Park, et al., "Analysis of Critical Flow Test Results for the Simulation of Loss of Coolant Accidents," Proceedings of KNS 2006 Spring Meeting, Korea, 2006.
- [14] K. Y. Choi et al., "MARS Input Data for 8 % State Calculation of the ATLAS," KAERI/TR-3046/2005, Korea Atomic Energy Research Institute, 2005.
- [15] S. Cho, et al., "Heat loss evaluation of the ATLAS facility," KNS 2009 Spring meeting, Jeju, 2009, May 22.
- [16] Y. S. Kim et al., "Startup Test Report of ATLAS," KAERI/TR-3330/2007, Korea Atomic Energy Research Institute, 2007.
- [17] The American Society of Mechanical Engineers, "Test Uncertainty," ASME PTC 19.1-1998, 1998.